

# Maximizing Coordination Capsule–Guest Polar Interactions in Apolar Solvents Reveals Significant Binding

David P. August, Gary S. Nichol, and Paul J. Lusby\*

**Abstract:** Guest encapsulation underpins the functional properties of self-assembled capsules yet identifying systems capable of strongly binding small organic molecules in solution remains a challenge. Most coordination capsules rely on the hydrophobic effect to ensure effective solution-phase association. In contrast, we show that using non-interacting anions in apolar solvents can maximize favorable interactions between a cationic  $\text{Pd}_2\text{L}_4$  host and charge-neutral guests resulting in a dramatic increase in binding strength. With quinone-type guests, association constants in excess of  $10^8 \text{ M}^{-1}$  were observed, comparable to the highest previously recorded constant for a metallocupramolecular capsule. Modulation of optoelectronic properties of the guests was also observed, with encapsulation either changing or switching-on luminescence not present in the bulk phase.

Supramolecular capsules appear at the forefront of research efforts because their propensity to partition whole molecules from the bulk phase produces interesting properties ranging from sensing<sup>[1]</sup> through catalysis<sup>[2]</sup> to the stabilization of reactive species.<sup>[3]</sup> With coordination systems, binding charge-neutral guests provides a notable challenge because of the competition with associated counter anions or cations.<sup>[4]</sup> As a result, polar solvents are typically favored as these stabilize the counter-charged species outside of the cavity.<sup>[5]</sup> Certain solvents, such as water, can also provide a strong and universal driving-force for guest encapsulation through solvophobic desolvation pathways.<sup>[6]</sup> However, metallo-organic capsules often possess a mix of hydrophobic and hydrophilic regions, usually large apolar aromatic surfaces linked by polar coordination vertices, such that binding can be difficult to predict and also requires a trade-off with possible favorable polar interactions.<sup>[7]</sup> Here we show that it is possible to attain significant binding, comparable with the strongest previously reported by a coordination capsule in water,<sup>[5a,8]</sup> almost  $10^9 \text{ M}^{-1}$  for a charge-neutral guest, by maximizing non-covalent interactions in apolar solvents.<sup>[9]</sup>

The system we selected to study was the  $\text{Pd}_2\text{L}_4$  capsule, **1**<sup>4+</sup> (Figure 1, left side), first reported by Hooley and co-workers,<sup>[10]</sup> in anticipation that a) the low charge would aid investigation in apolar solvents, b) the strong Pd-pyridine

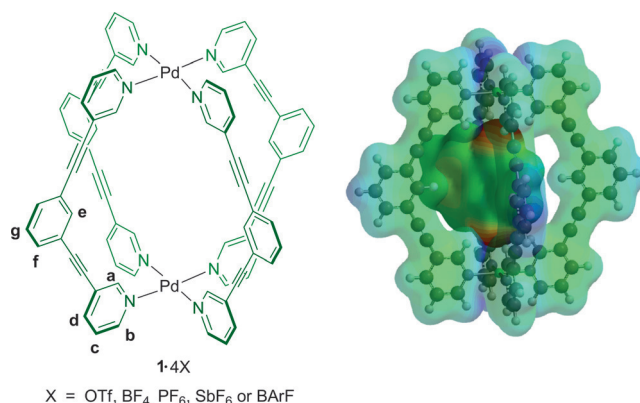


**Figure 1.** Left side: Chemical structure of the  $\text{Pd}_2\text{L}_4^{4+}$  cage, **1**<sup>4+</sup>. Right side: Energy-minimised model of naphthoquinone **G**<sup>1</sup> within the cavity of **1**<sup>4+</sup> showing attractive electrostatic surface potentials between the electron deficient CH regions of the capsule (shown in blue) and electron-rich areas provided by the guest (shown in red).

interactions would ensure the integrity of the anion-free cavity, and c) it would be possible to better the modest binding ( $< 20 \text{ M}^{-1}$ ) previously reported for various aromatic guests in DMSO.<sup>[10a]</sup> Molecular modeling also indicated that the *o*-pyridyl positions ( $\text{H}_a$ ) are polarized by the  $\text{Pd}^{\text{II}}$  ions creating pockets of H-bond donors that can form complementary interactions with guests such as quinones (Figure 1, right side).<sup>[11]</sup> Promisingly, when excess naphthoquinone, **G**<sup>1</sup>, was added to **1-4 OTf** in  $\text{CD}_3\text{CN}$ , the  $^1\text{H}$  NMR spectrum of the mixture showed significant changes when compared to the individual species (Figure 2). While the single set of host–

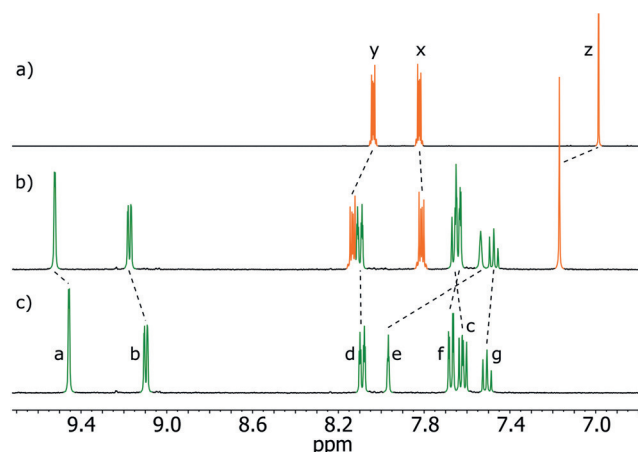


**Figure 2.** Partial  $^1\text{H}$  NMR spectra (500 MHz,  $\text{CD}_3\text{CN}$ , 300 K) of a) naphthoquinone, **G**<sup>1</sup>, only; b) a mixture of **1-4 OTf** with excess **G**<sup>1</sup>; c) **1-4 OTf** only. The lettering refers to those shown in Figures 1 and 3.

[\*] D. P. August, Dr. G. S. Nichol, Dr. P. J. Lusby  
EaStCHEM School of Chemistry, Joseph Black Building  
David Brewster Road, Edinburgh, EH9 3FJ (UK)  
E-mail: Paul.Lusby@ed.ac.uk

Supporting information, including synthesis, characterization data, X-ray analysis, and details of titration experiments, and the ORCID identification number(s) for the author(s) of this article can be found under <http://dx.doi.org/10.1002/ange.201608229>.

guest signals indicated that the interaction was dynamic relative to the NMR timescale, it was notable that the inside cage resonances ( $H_a$ ,  $H_e$ ) and two of the guest resonances ( $H_y$ ,  $H_z$ ) were most shifted. Also, whereas  $H_e$ ,  $H_y$  and  $H_z$  all moved upfield because of mutual shielding by host and guest aromatic surfaces,  $H_a$  was downfield shifted, supporting the initial supposition that binding would be driven by multiple  $CH\cdots O$  H-bonds.

We next sought to assess the strength of binding between  $G^1$  and  $1^{4+}$  (Table 1). Starting with  $1\cdot 4OTf$  in  $CD_3CN$ , plotting the change in chemical shifts ( $\Delta\delta$ ) of the host when titrated with  $G^1$  produced multiple curves that fitted a 1:1 binding isotherm, which gave a global association constant,  $K_a$ , of

**Table 1:** Association constants,  $K_a$ , for naphthoquinone,  $G^1$ , with various capsule ion-pairs,  $1\cdot 4X$ , in different solvents.<sup>[a]</sup>

Entry	X	Solvent	$K_a$ [ $M^{-1}$ ]	$\Delta G$ [kJ $mol^{-1}$ ]
1	OTf	$CD_3CN$	210	13.2
2	OTf	$CD_3OD$	26	8.1
3	OTf	$[D_8]THF$	290	14.1
4	OTf	$CD_2Cl_2$	1800	18.7
5	OTf	$CD_3NO_2$	2000	18.8
6	$BF_4$	$CD_3NO_2$	6500	21.7
7	$PF_6$	$CD_3NO_2$	13 000	23.5
8	$SbF_6$	$CD_3NO_2$	22 000	24.8
9	BArF	$CD_3NO_2$	50 000	26.8
10	BArF	$CD_3OD$	530	15.5
11	BArF	$CD_3CN$	1600	18.3
12	BArF	$CD_2Cl_2$	35 000 <sup>[b]</sup>	31.1

[a] Determined by  $^1H$  NMR titration, errors are estimated to be < 10%.

[b] Competitive  $^1H$  NMR titration with  $G^3$ .

$210\ M^{-1}$  (Table 1, Entry 1; see the Supporting Information for details). Encouraged that the affinity for  $G^1$  was ten-fold higher than the previous best guest,<sup>[10a]</sup> several different solvents were screened (Table 1, Entries 2–5), which indicated that apolar solvents promote better binding (Table 1, Entries 4,5). Surmising that even stronger binding was possibly being masked by tight ion-pairing, other capsule salts,  $1\cdot 4X$ , were then prepared either directly from the relevant  $Pd^{II}$  source ( $X^- = BF_4^-$ ) or by adding excess  $NaX$  or  $KX$  to  $1\cdot 4OTf$  ( $X^- = PF_6^-$ ,  $SbF_6^-$ ,  $BArF^-$  [ $BArF = B(3,5-(CF_3)_2C_6H_3)_4^-$ ]).<sup>[12]</sup> Non-capsule salts were removed by exploiting the low solubility of  $1\cdot 4X$  in either methanol or water, while  $^{19}F$  NMR spectroscopy confirmed anion metathesis. Interestingly, comparing the  $^1H$  NMR spectra of  $1\cdot 4X$  (see Figures S3, S27 in the Supporting Information) indicates that the stronger coordinating anions,  $OTf^-$  and  $BF_4^-$  in particular, are likely to reside within the cavity of the capsule, with internal signals  $H_a$  and  $H_e$  being notably deshielded by up to 0.2 ppm in the case of both  $1\cdot 4OTf$  and  $1\cdot 4BF_4$ .<sup>[13]</sup> The affinity of  $1^{4+}$  for the different anions was also qualitatively observed using ESI-MS;  $1\cdot 4OTf$  exhibited dominant 2+ and 3+ charge states with two and one associated anions, respectively, while the “naked”  $1^{4+}$  was the major ion with  $1\cdot 4BArF$  (Figures S28–32). Measuring the  $K_a$  for  $G^1$  with the additional ion-pair capsules  $1\cdot 4X$  in  $CD_3NO_2$ —the optimal solvent to balance solubility whilst maximizing favourable

interactions—revealed that, as anticipated, replacing  $OTf^-$  with weaker interacting anions (Table 1, Entries 5–9) increases the binding strength, with a significant 25-fold increase in the case of  $BArF^-$ .

The affinity of  $G^1$  for  $1\cdot 4BArF$  has also been measured in different solvents (Table 1, Entries 9–12). This analysis was more complicated with  $CD_2Cl_2$  as a solvent (Table 1, Entry 12) because of capsule signal broadening during the titration, indicating guest exchange was occurring close to the  $^1H$  NMR timescale. In this case,  $K_a$  was determined using a competitive binding experiment with a stronger, slow exchange guest (see below and Supporting Information).<sup>[14]</sup> The trend of increased binding with  $1\cdot 4OTf$  in solvents of decreasing polarity (Table 1, Entries 1–4) was mirrored by  $1\cdot 4BArF$  (Table 1, Entries 9–12), however, the latter produced globally higher affinities, from a factor of ten in more polar solvents through to a greater than 100-fold increase in  $CD_2Cl_2$ . Overall, the combination of weakly interacting anions and a non-polar solvent dramatically increases the  $K_a$  between  $1^{4+}$  and  $G^1$  by  $10^4$  (Table 1, Entry 2 vs. Entry 1) thus indicating that a major contribution to the binding free energy are the polar  $CH\cdots O$  H-bonds.

Using the optimized ion-pair and solvent combination ( $1\cdot 4BArF$  in  $CD_2Cl_2$ ), different potential guests were explored (Figure 3). Notably,  $G^{3-5}$  all showed slow in-out kinetics, which was most apparent with  $G^5$  because of the reduction in capsule symmetry caused by the different benzo

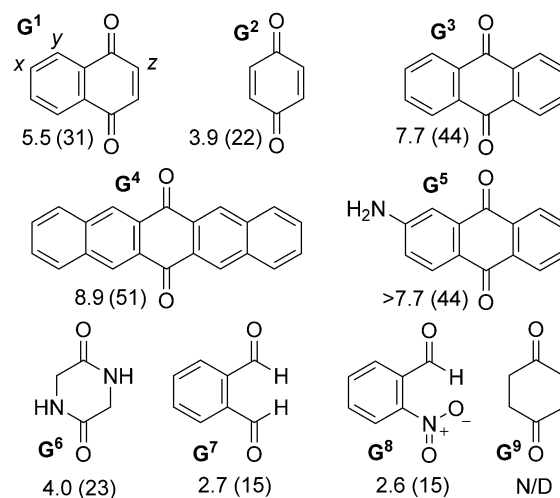


**Figure 3.** The  $\log K_a$  values for selected molecules, with binding strength energies (kJ  $mol^{-1}$ ) shown in parenthesis. Association constants measured in  $CD_2Cl_2$  using  $1\cdot 4BArF$ , except  $G^6$ , which was obtained in  $CD_3CN$ .

rings of the guest (Figure S35). Addition of sub-stoichiometric  $G^{3-5}$  to  $1\cdot 4BArF$  also revealed that they were very tight binders as no free guest was detectable at concentrations above  $50\ \mu M$ .<sup>[15]</sup> Strong association was also evident by preservation of the inclusion complexes under ESI-MS conditions (Figures S57–59). Consequently, association constants were obtained using  $^1H$  NMR competitive titration experiments;  $K_a$  for  $G^3$  was measured using a large excess of

the fast exchange guest  $\mathbf{G}^2$ , while  $\mathbf{G}^4$  was competed against  $\mathbf{G}^3$  (see Supporting Information). Attempts to obtain a binding constant for  $\mathbf{G}^5$  using competitive binding produced data of insufficient quality, however, the same experiment showed it was better than  $\mathbf{G}^3$ .

With the quinone series ( $\mathbf{G}^1$ – $\mathbf{G}^5$ ), increasing the number of fused aromatic rings results in a significant increase in  $K_a$ . The difference between  $\mathbf{G}^1$  vs.  $\mathbf{G}^2$  and  $\mathbf{G}^2$  vs.  $\mathbf{G}^3$  are fairly similar, with each additional aromatic ring adding about  $10 \text{ kJ mol}^{-1}$  to the binding strength.<sup>[16]</sup> These energetic contributions are likely a result of additional edge-to-face interactions ( $\text{CH}\cdots\pi$  H-bonds,<sup>[9a]</sup> see below), which is consistent with the significant shielding of  $\text{H}_c$  observed by  $^1\text{H}$  NMR spectroscopy following host–guest complexation. With pentaenedione,  $\mathbf{G}^4$ , the extra two rings produce a smaller increase, perhaps not unsurprisingly as these protrude further into the void between adjacent ligands. Nonetheless, the  $\log K_a$  of 8.9 for  $\mathbf{G}^4$  is, as far as we are aware, comparable to the highest for a charge neutral guest inside a coordination capsule. The crystal structure of  $[\mathbf{G}^4\subset\mathbf{1}]\text{4OTf}$  has also been obtained, using single crystals grown from  $\text{CH}_3\text{CN}$  and  $\text{Et}_2\text{O}$  (Figure 4).<sup>[17]</sup>

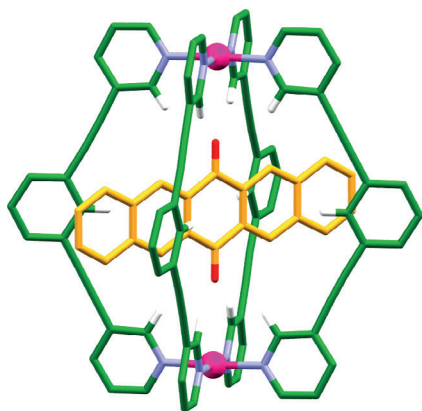


**Figure 4.** X-ray crystal structure of  $[\mathbf{G}^4\subset\mathbf{1}]\text{4OTf}$  (counteranions, solvent and non-interacting H atoms omitted for clarity). Color code: carbon of  $\mathbf{1}^{4+}$ , green; carbon of  $\mathbf{G}^4$ , orange; hydrogen, white; nitrogen, blue; oxygen, red; palladium, magenta.

The solid state structure confirms the solution binding model with the oxygen atoms of  $\mathbf{G}^4$  clearly located in the two pockets of four  $\text{H}_a$  atoms, with C–O distances ranging from 3.3 to  $3.8 \text{ \AA}$ , indicating multiple  $\text{CH}\cdots\text{O}$  H-bonds. Edge-to-face interactions between the extended aromatic surface of  $\mathbf{G}^4$  and the four  $\text{H}_c$  atoms are also apparent (see above). In addition to quinones,  $\mathbf{1}^{4+}$  also binds other guests with suitably disposed H-bond acceptor groups (e.g.  $\mathbf{G}^{6-8}$ ). The  $\log K_a$  of 4.0 for  $\mathbf{G}^6$  was measured in  $\text{CD}_3\text{CN}$  to alleviate problems of intermediate exchange; a comparison with  $\mathbf{G}^1$  under similar conditions (Table 1, entry 11) is consistent with the better H-bond acceptor properties of amides versus enones, not least considering  $\mathbf{G}^6$  lacks the additional benzo ring that adds  $10 \text{ kJ mol}^{-1}$  to the binding strength of  $\mathbf{G}^1$ . A further interesting comparison can also be made to the classic tetraamide macrocycle reported by Hunter and co-workers,<sup>[18]</sup> which binds  $\mathbf{G}^2$ ,  $\mathbf{G}^6$  and  $\mathbf{G}^9$ . Whereas the  $K_a$  for  $[\mathbf{G}^2\subset\mathbf{1}]^{4+}$  is an order

of magnitude higher than the tetraamide macrocycle under similar conditions, and a solvent/anion adjusted value for  $[\mathbf{G}^6\subset\mathbf{1}]^{4+}$  would be at least comparable with the covalent host, in contrast  $\mathbf{G}^9$  shows no evidence of encapsulation inside  $\mathbf{1}^{4+}$ .<sup>[19]</sup> A molecular model of  $\mathbf{G}^9$  revealed that the preferred chair conformation results in only a marginally smaller distance between H-bond acceptor oxygen atoms in comparison to  $\mathbf{G}^2$  ( $\Delta(\text{O}\cdots\text{O}) = 0.1 \text{ \AA}$ ). Instead, the lack of binding could possibly be due to the non-linear orientation of carbonyl groups, coupled to the relative rigidity of the metallosupramolecular framework, thus not allowing an optimal arrangement of H-bonding interactions with both sets of CH donor pockets.

The optoelectronic properties of guests  $\mathbf{G}^{4-5}$  are modulated upon encapsulation within  $\mathbf{1}^{4+}$ . With  $\mathbf{G}^5$  both the  $\lambda_{\text{max}}$  of the absorption and emission spectra are redshifted with respect to the free guest, by 70 and 34 nm, respectively (see Figures S66), a possible consequence of the LUMO being stabilized by H-bonding to the capsule. Similar yet even more dramatic effects are seen with  $\mathbf{G}^4$ . Whereas both  $\mathbf{1}\cdot\mathbf{4BARF}$  and  $\mathbf{G}^4$  are virtually colorless to the naked eye under ambient lighting,  $[\mathbf{G}^4\subset\mathbf{1}]\text{4BARF}$  is clearly yellow (Figure 5, left side,

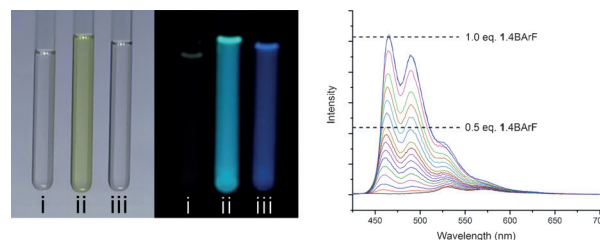


**Figure 5.** Left side: Images of  $100 \mu\text{M}$   $\text{CD}_2\text{Cl}_2$  solutions of i)  $\mathbf{G}^4$ ; ii)  $[\mathbf{G}^4\subset\mathbf{1}]\text{4BARF}$ ; iii)  $\mathbf{1}\cdot\mathbf{4BARF}$  under ambient lighting (left) and under a 365 nm UV lamp (right). Right side: Fluorescence titration of  $\mathbf{1}\cdot\mathbf{4BARF}$  into  $100 \mu\text{M}$  of  $\mathbf{G}^4$  in  $\text{CH}_2\text{Cl}_2$  with excitation at 412 nm (isosbestic point of  $\mathbf{G}^4$  and  $[\mathbf{G}^4\subset\mathbf{1}]\text{4BARF}$ ). A quantum yield enhancement factor of 15.6 was calculated from the relative peak intensities of  $\mathbf{G}^4$  and  $[\mathbf{G}^4\subset\mathbf{1}]\text{4BARF}$ . No further increase in emission intensity was observed upon addition of excess  $\mathbf{1}\cdot\mathbf{4BARF}$ .

left). When held under a UV lamp, the difference is even more stark, with  $[\mathbf{G}^4\subset\mathbf{1}]\text{4BARF}$  showing strong emission whereas  $\mathbf{G}^4$  alone shows little (Figure 5, left side, right). The switch-on emission of the host–guest complex has also been confirmed spectroscopically, both by titrating  $\mathbf{1}\cdot\mathbf{4BARF}$  into  $\mathbf{G}^4$  (Figure 5, right side) and also  $\mathbf{G}^4$  into  $\mathbf{1}\cdot\mathbf{4BARF}$  (Figure S63,64). In both cases, the emission intensity increases until a 1:1 ratio of  $\mathbf{1}\cdot\mathbf{4BARF}$  and  $\mathbf{G}^4$  is reached, where after it remains constant, strongly indicating that the luminescence is due to the formation of  $[\mathbf{G}^4\subset\mathbf{1}]\text{4BARF}$ . While many coordination cages have been shown to quench the emission of guests, due to heavy-atom effects and/or charge-transfer processes, those that either maintain or even enhance the optoelectronic properties of the encapsulated species are rare.<sup>[20]</sup> In the case of  $[\mathbf{G}^4\subset\mathbf{1}]\text{4BARF}$ , we likely attribute the increase in fluorescence with respect to the free guest due to preventing the formation of weakly-emissive aggregates.<sup>[20a]</sup>



In conclusion, we have shown that minimizing the competitive interactions between a charged cationic cage and its associated anions can lead to a dramatic increase in the strength of charge-neutral guest binding in apolar solvents, giving association constants comparable to the highest previously observed for a metallocsupramolecular capsule system. We are currently investigating how such electronic manipulation of guest molecules can be exploited for various applications.

## Acknowledgements

We thank the University of Edinburgh for a Principal's Career Development Scholarship (D.P.A.).

**Keywords:** coordination capsules · host–guest systems · non-coordinating anions · quinones · self-assembly

**How to cite:** *Angew. Chem. Int. Ed.* **2016**, *55*, 15022–15026  
*Angew. Chem.* **2016**, *128*, 15246–15250

- [1] For representative examples, see a) A. Suzuki, K. Kondo, Y. Sei, M. Akita, M. Yoshizawa, *Chem. Commun.* **2016**, 52, 3151–3154; b) P. D. Frischmann, V. Kunz, F. Würthner, *Angew. Chem. Int. Ed.* **2015**, *54*, 7285–7289; *Angew. Chem.* **2015**, *127*, 7393–7397; c) C. He, J. Wang, P. Wu, L. Jia, Y. Bai, Z. Zhangab, C. Duan, *Chem. Commun.* **2012**, 48, 11880–11882; d) O. Chepelin, J. Ujma, X. Wu, A. M. Z. Slawin, M. B. Pitak, S. J. Coles, J. Michel, A. C. Jones, P. E. Barran, P. J. Lusby, *J. Am. Chem. Soc.* **2012**, *134*, 19334–19337.
- [2] For representative examples, see a) P. Howlader, P. Das, E. Zangrando, P. S. Mukherjee, *J. Am. Chem. Soc.* **2016**, *138*, 1668–1676; b) W. Cullen, M. C. Misuraca, C. A. Hunter, N. H. Williams, M. D. Ward, *Nat. Chem.* **2016**, *8*, 231–236; c) D. M. Kaphan, M. D. Levin, R. G. Bergman, K. N. Raymond, F. D. Toste, *Science* **2015**, *350*, 1235–1238; d) A. G. Salles, S. Zarra, R. M. Turner, J. R. Nitschke, *J. Am. Chem. Soc.* **2013**, *135*, 19143–19146; e) T. Murase, Y. Nishijima, M. Fujita, *J. Am. Chem. Soc.* **2012**, *134*, 162–164.
- [3] For representative examples, see a) M. Yamashina, Y. Sei, M. Akita, M. Yoshizawa, *Nat. Commun.* **2014**, *5*, 4662; b) S. Horiuchi, T. Murase, M. Fujita, *J. Am. Chem. Soc.* **2011**, *133*, 12445–12447; c) P. Mal, B. Breiner, K. Rissanen, J. R. Nitschke, *Science* **2009**, *324*, 1697–1699; d) T. Iwasawa, R. J. Hooley, J. Rebek, Jr., *Science* **2007**, *317*, 493–496.
- [4] For examples of counteranion/cation binding, see a) M. D. Johnstone, E. K. Schwarze, J. Ahrens, D. Schwarzer, J. J. Holstein, B. Dittich, F. M. Pfeffer, G. H. Clever, *Chem. Eur. J.* **2016**, *22*, 10791–10795; b) S. Freye, J. Hey, A. Torras-Galán, D. Stalke, R. Herbst-Irmer, M. John, G. H. Clever, *Angew. Chem. Int. Ed.* **2012**, *51*, 2191–2194; *Angew. Chem.* **2012**, *124*, 2233–2237; c) I. A. Riddell, M. M. J. Smulders, J. K. Clegg, Y. R. Hristova, B. Breiner, J. D. Thoburn, J. R. Nitschke, *Nat. Chem.* **2012**, *4*, 751–756; d) C. R. K. Glasson, J. K. Clegg, J. C. McMurry, G. V. Meehan, L. F. Lindoy, C. A. Motti, B. Moubaraki, K. S. Murray, J. D. Cashion, *Chem. Sci.* **2011**, *2*, 540–543; e) Y. R. Hristova, M. M. J. Smulders, J. K. Clegg, B. Breiner, J. R. Nitschke, *Chem. Sci.* **2011**, *2*, 638; f) G. H. Clever, S. Tashiro, M. Shionoya, *Angew. Chem. Int. Ed.* **2009**, *48*, 7010–7012; *Angew. Chem.* **2009**, *121*, 7144–7146; g) J. S. Fleming, K. L. V. Mann, C.-A. Carraz, E. Psillakis, J. C. Jeffery, J. A. McCleverty, M. D. Ward, *Angew. Chem. Int. Ed.* **1998**, *37*, 1279–1281; *Angew. Chem.* **1998**, *110*, 1315–1318; h) D. L. Caulder, R. E. Powers, T. N. Parac, K. N. Raymond, *Angew. Chem. Int. Ed.* **1998**, *37*, 1840–1843; *Angew. Chem.* **1998**, *110*, 1940–1943; i) M. Fujita, D. Oguro, M. Miyazawa, H. Oka, K. Yamaguchi, K. Ogura, *Nature* **1995**, *378*, 469.
- [5] For examples of charge neutral-guest binding, see a) W. Cullen, S. Turega, C. A. Hunter, M. D. Ward, *Chem. Sci.* **2015**, *6*, 2790–2794; b) P. R. Symmers, M. J. Burke, D. P. August, P. I. T. Thomson, G. S. Nichol, M. R. Warren, C. J. Campbell, P. J. Lusby, *Chem. Sci.* **2015**, *6*, 756–760; c) S. Turega, W. Cullen, M. Whitehead, C. A. Hunter, M. D. Ward, *J. Am. Chem. Soc.* **2014**, *136*, 8475–8483; d) J. L. Bolliger, T. K. Ronson, M. Ogawa, J. R. Nitschke, *J. Am. Chem. Soc.* **2014**, *136*, 14545–14553; e) N. Kishi, Z. Li, Y. Sei, M. Akita, K. Yoza, J. S. Siegel, M. Yoshizawa, *Chem. Eur. J.* **2013**, *19*, 6313–6320; f) F. Schmitt, J. Freudenreich, N. P. E. Barry, L. Juillerat-Jeanneret, G. Süß-Fink, B. Therrien, *J. Am. Chem. Soc.* **2012**, *134*, 754–757; g) P. Mal, D. Schultz, K. Beyeh, K. Rissanen, J. R. Nitschke, *Angew. Chem. Int. Ed.* **2008**, *47*, 8297–8301; *Angew. Chem.* **2008**, *120*, 8421–8425; h) S. M. Biro, R. G. Bergman, K. N. Raymond, *J. Am. Chem. Soc.* **2007**, *129*, 12094–12095; i) T. Kusakawa, M. Fujita, *Angew. Chem. Int. Ed.* **1998**, *37*, 3142–3144; *Angew. Chem.* **1998**, *110*, 3327–3329.
- [6] a) F. Biedermann, W. M. Nau, H.-J. Schneider, *Angew. Chem. Int. Ed.* **2014**, *53*, 11158–11171; *Angew. Chem.* **2014**, *126*, 11338–11352; b) L. Yang, C. Adam, S. L. Cockroft, *J. Am. Chem. Soc.* **2015**, *137*, 10084–10087.
- [7] M. Whitehead, S. Turega, A. Stephenson, C. A. Hunter, M. D. Ward, *Chem. Sci.* **2013**, *4*, 2744–2751.
- [8] For strong binding of charge-neutral guests by a cofacial porphyrin dimeric coordination capsule in mixed dichloromethane/methanol, see T. Nakamura, H. Ube, M. Shionoya, *Angew. Chem. Int. Ed.* **2013**, *52*, 12096–12100; *Angew. Chem.* **2013**, *125*, 12318–12322.
- [9] For other examples of maximizing non-covalent interactions in non-polar solvents, see a) S. L. Cockroft, C. A. Hunter, *Chem. Commun.* **2006**, 3806–3808; b) G. M. Prentice, S. I. Pascu, S. V. Filip, K. R. West, G. D. Pantoş, *Chem. Commun.* **2015**, 51, 8265–8268.
- [10] a) P. Liao, B. W. Langloss, A. M. Johnson, E. R. Knudsen, F. S. Tham, R. R. Julian, R. J. Hooley, *Chem. Commun.* **2010**, 46, 4932–4934; For cisplatin guest binding in a structurally similar Pd<sub>2</sub>L<sub>4</sub> cage system, see b) J. E. M. Lewis, E. L. Gavey, S. A. Cameron, J. D. Crowley, *Chem. Sci.* **2012**, *3*, 778–784; For recent reviews on Pd<sub>2</sub>L<sub>4</sub> capsules, see c) M. Han, D. M. Engelhard, G. H. Clever, *Chem. Soc. Rev.* **2014**, *43*, 1848–1860; d) A. Schmidt, A. Casini, F. E. Kühn, *Coord. Chem. Rev.* **2014**, *275*, 19–36.
- [11] For examples of metal ion polarised CH H-bonding, see a) A. J. Metherell, W. Cullen, A. Stephenson, C. A. Hunter, M. D. Ward, *Dalton Trans.* **2014**, 43, 71–84; For examples of similar host-guest interactions in coordination cages, see Refs. [4a, 5a, 8].
- [12] For recent examples of organocatalysis using cationic H-bond donors that employ weakly coordinating anions, see a) W. Xu, M. Arieno, H. Löw, K. Huang, X. Xie, T. Cruchter, Q. Ma, J. Xi, B. Huang, O. Wiest, L. Gong, E. Meggers, *J. Am. Chem. Soc.* **2016**, *138*, 8774–8780; b) Y. Fan, S. R. Kass, *Org. Lett.* **2016**, *18*, 188–191; c) S. Shirakawa, S. Liu, S. Kaneko, Y. Kumatabara, A. Fukuda, Y. Omagari, K. Maruoka, *Angew. Chem. Int. Ed.* **2015**, *54*, 15767–15770; *Angew. Chem.* **2015**, *127*, 15993–15996.
- [13] For anions such as OTf and BF<sub>4</sub>, it is likely that strong coulombic attraction is supplemented by a well defined secondary coordination sphere that involves multiple *o*-pyridyl CH...O or CH...F H-bonds. For the X-ray structure of a similar primary and secondary coordination sphere, see a) C. Bianchini, J. Filippi, A. Lavacchi, W. Oberhauser, *Eur. J. Inorg. Chem.* **2011**, 1797–1805. With 1-4OTf and 1-4BF<sub>4</sub>, it is anticipated that, in solution, two anions interact with the external *o*-pyridyl pockets (noticeable

- shifts of  $H_b$  in the  $^1\text{H}$  NMR spectra are observed, Figure S27), however, it is suspected that both the coulombic repulsion and size limitation of the capsules cavity means that only one of the internal *o*-pyridyl sites is occupied at any one time. Similar anion binding within capsules has been observed in the solid state, see Ref. [9a] and also, b) J. E. M. Lewis, J. D. Crowley, *Supramol. Chem.* **2014**, 26, 173–181.
- [14] While the errors associated with binding constants determined by competitive titration experiments are likely to be greater than 10%, such uncertainty is offset by the significant difference in  $K_a$  values, see Figure S38.
- [15] At concentrations less than 50  $\mu\text{M}$ ,  $\mathbf{1}^{4+}$  starts to disassemble, see Figure S33.
- [16] A slightly larger increase in the binding strength is observed between the first and second additional benzo groups (9 vs. 12  $\text{kJ mol}^{-1}$ ), possibly indicating that for  $\mathbf{G}^2$  there is free rotation of the guest in the cavity around the  $C_2$  axis that connects both CO groups. With  $\mathbf{G}^1$  the additional CH- $\pi$  interactions would be partially offset by the loss in entropy caused by the lack of rotation for this larger guest, hence the subsequent difference between  $\mathbf{G}^1$  and  $\mathbf{G}^3$  is larger.
- [17] CCDC 1492902 [ $\mathbf{G}^4\text{C1}$ ]4OTf contains the supplementary crystallographic data for this paper. These data can be obtained free of charge from The Cambridge Crystallographic Data Centre.
- [18] H. Adams, F. J. Carver, C. A. Hunter, N. J. Osborne, *Chem. Commun.* **1996**, 2529–2530.
- [19] While small changes to the  $^1\text{H}$  NMR signals of  $\mathbf{1}^{4+}$  signals were observed upon titration with  $\mathbf{G}^9$ , attempts to fit this data to a 1:1 binding model gave a meaningless  $K_a$  value ( $0.1 \pm 96 \text{ M}^{-1}$ ). We attribute the small changes to other possible, weak binding modes, such as interactions with the external *o*-pyridyl H-bond donors.
- [20] a) K. Ono, J. K. Klosterman, M. Yoshizawa, K. Sekiguchi, T. Tahara, M. Fujita, *J. Am. Chem. Soc.* **2009**, 131, 12526–12527; b) P. P. Neelakandan, A. Jiménez, J. R. Nitschke, *Chem. Sci.* **2014**, 5, 908–915; c) M. Yamashina, M. M. Sartin, Y. Sei, M. Akita, S. Takeuchi, T. Tahara, M. Yoshizawa, *J. Am. Chem. Soc.* **2015**, 137, 9266–9269.

Received: August 23, 2016

Revised: September 9, 2016

Published online: November 3, 2016